Bioorganic & Medicinal Chemistry Letters 26 (2016) 602–608

Contents lists available at ScienceDirect

Bioorganic & Medicinal Chemistry Letters

journal homepage: www.elsevier.com/locate/bmcl

Promising applications in drug delivery systems of a novel β-cyclodextrin derivative obtained by green synthesis

Agustina García, Darío Leonardi *, María C. Lamas *

IQUIR-CONICET, Facultad de Ciencias Bioquímicas y Farmacéuticas, Universidad Nacional de Rosario, Suipacha 531, 2000 Rosario, Santa Fe, Argentina
Área Técnica Farmacéutica, Facultad de Ciencias Bioquímicas y Farmacéuticas, Universidad Nacional de Rosario, Suipacha 531, 2000 Rosario, Santa Fe, Argentina

ARTICLE INFO

Article history:
Received 22 September 2015
Revised 16 November 2015
Accepted 19 November 2015
Available online 20 November 2015

Keywords:
Cyclodextrin derivatives
Green synthesis
Inclusion complex

ABSTRACT

An efficient and green method has been developed for the synthesis of succinyl-β-cyclodextrin in aqueous media obtaining very good yield. Acidic groups have been introduced in the synthesized carrier molecule to improve the guest–host affinity.

To evaluate the suitability of the novel excipient focused to develop oral dosage forms, albendazole, a BSC class II compound, was chosen as a model drug.

The β-cyclodextrin derivative and the inclusion complex were thoroughly characterized in solution and solid state by phase solubility studies, FT-IR spectroscopy, SEM, XRD, ESI-MS, DSC, 1D ^{1}H NMR, 1D ^{13}C NMR, selective 1D TOCSY, 2D COSY, 2D HSQC, 2D HMBC and ROESY NMR spectroscopy. Phase solubility studies indicated that both of them β-cyclodextrin and succinyl-β-cyclodextrin formed 1:1 inclusion complexes with albendazole, and the stability constants were 68 M^{-1} (β-cyclodextrin), 437 M^{-1} (succinyl-β-cyclodextrin), respectively.

Water solubility and dissolution rate of albendazole were significantly improved in complex forms. Thus, the succinyl-β-cyclodextrin derivative could be a promising excipient to design oral dosage forms.

More than 1.5 billion people are infected with soil-transmitted helminth infections being a major cause of morbidity and mortality worldwide. Unprecedented efforts are now being made to control these infections by means of health education, improved hygiene and sanitation, provision of safe water, vector control, and selective chemotherapy using effective anthelmintic agents, including albendazole (ABZ).[1]

ABZ, a benzimidazole carbamate, presents basic functional groups and has a broad anthelmintic spectrum.[2] ABZ is used to treat several systemic helminthic diseases such as trichinellosis, hydatidosis and cysticercosis. Despite the fact that ABZ presents high lipophilicity (log*P* of 2.55), its poor water solubility (0.001 mg/mL) certainly produces a variable oral absorption.[2–4] However, high doses and long treatment are required in the most recent cases of helminth infections, due mainly to the poor solubility and absorption. Several procedures have been previously carried out to improve the aqueous solubility and dissolution rate of ABZ including the preparation of solid dispersions, microencapsulation, nanosuspensions, nanosize liposomes and inclusion complexes with cyclodextrins (CDs).[5–10]

CDs are cyclic oligosaccharides containing six, seven or eight D-glucopyranose units linked by α-(1,4) glucosidic bonds, corresponding to α, β and γ CD, respectively.[11–14] Each glucopyranose unit contains three free hydroxyl groups, differing both in their availability and reactivity. Primary and secondary hydroxyl groups in CDs are located on the lower and upper rim of the torus-shaped cavity.[15] The structure of CDs shows hydrophilic outer surface and hydrophobic inner cavity, which, in turn, allows a variety of hydrophobic compounds to be incorporated into their cavities, via host–guest complexation,[16–19] increasing the solubility, stability and bioavailability of bioactive compounds.[11,20,21]

Particularly, β-CD presents a low aqueous solubility (18.5 mg/mL) due to the formation of an internal hydrogen-bond network between the secondary hydroxyl groups restricting its pharmaceutical application. The random substitution of the hydroxyl groups of β-CD produces an important increase in its solubility due to the achievement of statistically substituted material formed by many isomeric components, and also prevents its crystallization.[16,22–24]

The type, number and position of the substituent's molecules of CDs, have shown a direct relationship between the affinity of the CD derivative and the guest. Therefore, the host–guest affinity could improve when the CD and the drug carry opposite charges.[25] Additionally, the affinity between β-CD and model drugs also plays

* Corresponding authors. Tel.: +54 341 4804592; fax: +54 341 4370477.
E-mail addresses: leonardi@iquir-conicet.gov.ar, dleonard@fbioyf.unr.edu.ar (D. Leonardi), lamas@iquir-conicet.gov.ar, mlamas@fbioyf.unr.edu.ar (M.C. Lamas).

http://dx.doi.org/10.1016/j.bmcl.2015.11.067
0960-894X/

a major role in modifying the apparent solubility and the drug release rate.[25,26]

Several derivatives of CDs have been synthesized for different purposes.[27–29] Modified β-CDs such as 6-*O*-succinyl-β-CD or 6-*N*-succinyl-β-CD, were synthesized and then employed as chiral selectors in capillary electrophoresis or in peptide synthesis of trypsin.[30,31] CDs derivatives, such as sulfobutylated, sulfobutyl ether, hydroxypropyl, methyl-CDs have attracted considerable attention in pharmaceutical fields.[29,32–34]

Thus, the goal of this work was to report a simple and green method, to synthesize a succinyl-β-CD (S-β-CD) derivative and to thoroughly investigate the physicochemical properties and behavior ABZ inclusion complex.

In recent years due to environmental issues, biodegradable and eco-friendly conditions for further pharmaceutical application have increased considerably attention. The main key in green synthesis of CDs derivatives has been the solvent choice, avoiding the use of organic solvents and highlighting the aqueous conditions in the chemical reaction process.

The synthesis of S-β-CD has been done following very mild conditions, using low-cost and eco-friendly materials in a very good yield (76.2%). Succinic acid (8.12 mmol, 959 mg) was dissolved in water (0.8 mL). Sodium hypophosphite monohydrate (SHP) (0.58 mmol, 63 mg) and β-CD (1.16 mmol, 1316 mg) were incorporated to the succinic acid solution. The reaction mixture was refluxed at 118 °C for 5 h. Afterwards, the reaction product was precipitated with absolute ethanol (20 mL)[35] while the un-reacted succinic acid and the reminder SHP were maintained in the solution. The precipitated was purified by washing with ethanol until the pH of the supernatant was neutral. The product was dried at 60 °C for 24 h.

A complete NMR study was carried out to determine the S-β-CD derivative substitution pattern. This compound was analyzed by one-dimensional NMR experiments (^{1}H NMR, ^{13}C NMR and ^{1}H-TOCSY) and bi-dimensional NMR experiments (^{1}H–^{1}H COSY, ^{1}H–^{13}C HSQC and ^{1}H–^{13}C HMBC). NMR spectra were recorded on a Bruker Avance 300 instrument (Karlsruhe, Germany). The chemical shifts were referenced to the internal reference of D_2O (δ 4.7 ppm). Experiments were performed on 24 mM S-β-CD samples in D_2O. The assignment of the ^{1}H and ^{13}C peaks are exhibited in the horizontal and vertical projection of HSQC spectrum, respectively (Figure 1). These results were obtained from analysis of 1D ^{1}H NMR, 1D ^{13}C NMR, selective 1D TOCSY, 2D COSY, 2D HSQC and 2D HMBC spectra. Two peaks are observed in the ^{1}H NMR spectrum at 4.48 and 4.16 ppm which present cross-peaks with the ^{13}C peak at 64.23 ppm on the 2D HSQC spectrum. Due to multiplicity-edited HSQC spectra differentiate CH (black) from CH_2 (grey) correlations, it is clear that the signals mentioned above correspond to the substituted nuclei at 6-position ($X6_{sub}$). In agreement with previous works, the directly substituted carbons ($C6_{sub}$) were shifted 4.03 ppm downfield relative to their unsubstituted counterparts while the neighboring carbons (C5′) were shifted upfield 2.14 ppm. Protons attached to directly substituted carbons ($H6_{sub}$ a,b) were shifted downfield by 0.37–0.69, while protons on neighboring carbons (C5′) were shifted downfield 0.19 ppm. In Figure 1, the presence of signals corresponding to unsubstituted nuclei at 6-position denote a partial substitution of the S-β-CD. Selective 1D TOCSY is able to establish the correlation between protons that sit within the same spin system. Thus, the 1D TOCSY spectrum with varied duration of the propagation period could give subspectra of each D-glucose residue depending on the irradiated nucleus. The selective irradiation of ^{1}H at 4.48 and 4.17 ppm produced a 1D TOCSY spectrum that evidenced a spin system involving a proton with a resonance at 3.97 ppm. Also, this signal presented cross-peak on the 2D COSY spectrum with the signal corresponded to $H6_{sub}$ a,b verifying that these protons are H5

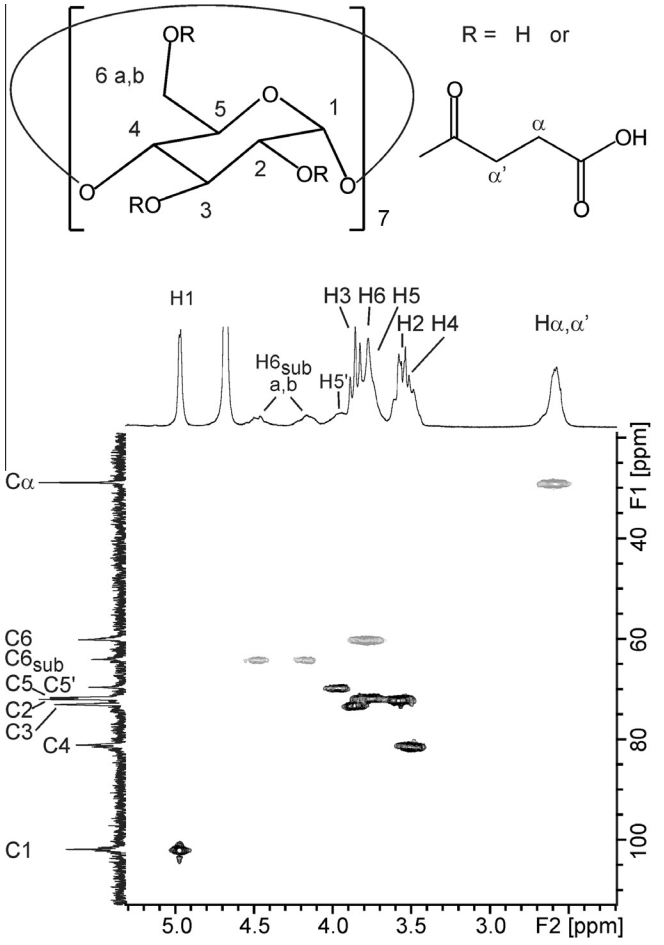

Figure 1. Multiplicity-edited ^{1}H–^{13}C HSQC spectrum of the S-β-CD. Positive CH correlations are plotted in black and negative CH_2 correlations are plotted in gray. The assignment of the ^{1}H and ^{13}C signals are shown in the horizontal and vertical projection, respectively.

neighbors (H5′) to the H6 protons attached to substituted carbons (data not shown). The average degree of substitution (DS) could be quantified from the proton peak areas. As could be seen in Figure 1, $H6_{sub}$ a,b; Hα–α′ non presenting overlapping. Thus, the DS could be determined by comparing the sum of these three peaks (which integrated 6 protons) to the peak area of H1 (which integrated 1 proton). The DS obtained from ^{1}H NMR was 2.86 per CD molecule.

High Resolution Mass spectra were recorded on a Bruker micrOTOF-Q II spectrometer (Bruker-Daltonics, Bremen, Germany). ESI-MS conditions were optimized in order to observe the derivative. The spectrometer parameters were set as follows: ESI (negative ion mode), collision energy: −5 eV, spray voltage 2.8 kV, nebulizer: 0.4 bar, dry heater: 180 °C, drying gas flow rate: 4.0 L/min, end plate offset: −500 V, set collision Cell RF: 750.0 Vpp. The S-β-CD was dissolved in a formic acid solution (0.4% v/v) and the spectra were obtained in the range m/z 50–3000. The average degree of substitution was estimated from the peak intensities, according to Eq. 1:

$$DS = \frac{\sum_i I_i DS_i}{\sum_i I_i} \quad (1)$$

where I_i is the intensity of the ith peak and DS_i is the degree of substitution corresponding to the ith peak. The partial ESI-mass spectrum of S-β-CD derivative recorded in the negative mode is shown in Figure 2. In this spectrum the peaks related to doubly charged species present a normal distribution. According to the

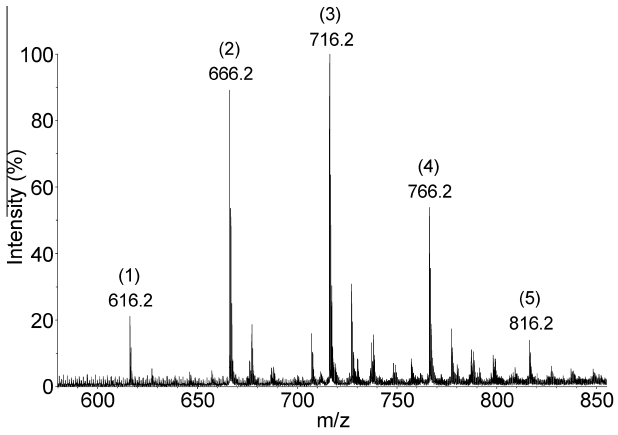

Figure 2. ESI-MS spectrum of S-β-CD.

deconvolution analysis of ions at *m*/*z* 616.2, 666.2, 716.2, 766.2 and 816.2, those peaks corresponded to doubly charged species and corresponded to the exact values of masses 1234.4, 1334.4, 1434.4, 1534.4 and 1634.4. Based on these results, five derivatives were found on this spectrum bearing from one to five succinyl substituents having an average DS of 2.83 per CD molecule (calculated according to Eq. 1). This result was consistent with the obtained by NMR.

Thereafter, to evaluate the relationship between the ABZ and the novel β-CD derivative, phase solubility studies have been done following these conditions:[7] Excess amounts of ABZ were added to 10 mL of water (pH = 6.3) or to an aqueous solution of β-CD or S-β-CD (10–60 mM). The samples were then shaken at 25.0 ± 0.5 °C for 72 h and filtered through a 0.45 μm membrane filter (Advantec MFS, Inc.). ABZ concentrations were determined spectrophotometrically at 292 nm. Each experiment was performed in triplicate. The complex formation constants (*K*f), were calculated by Eq. 2, which was reported by Higuchi and Connors.[36]

$$Kf = \frac{S}{S_0}(1 - S) \quad (2)$$

where S_0 is the ABZ solubility and *S* is the slope obtained by plotting the phase-solubility diagrams (data not shown).

The obtained *K*f values were 68 M^{-1} (β-CD) and 437 M^{-1} (S-β-CD). The linear relationship between ABZ and the S-β-CD fitted an A_L-type system.[36] This type of curves indicated the formation of soluble 1:1 type inclusion complex. The *K*f value suggested a relatively stable complex. The higher stability of ABZ:S-β-CD respect to ABZ:β-CD could be due to an interaction between the acidic groups of the S-β-CD and the basic groups of ABZ. Based on the data presented above, the systems ABZ:S-β-CD were formulated in a equimolar ratio.

Preparation of inclusion complexes and physical mixtures: Inclusion complexes: ABZ (0.56 mmol), S-β-CD (0.56 mmol) or β-CD (0.56 mmol) were dissolved in 30 mL of acetic acid (30% v/v). The resulting solution was spray-dried (SD) using a Mini Spray Dryer Buchi B-290 (Flawil, Switzerland) under the following conditions: inlet temperature: 130 °C, outlet temperature: 70 °C, air flow: 38 m^3/h, feed: 5 mL/min and aspirator set: 100%. Physical mixtures (PMs) were prepared by mixing ABZ, S-β-CD or β-CD in a mortar in equimolar ratio for 10 min.

ROESY NMR experiment provides information for investigating inter and intra molecular interactions and it is relevant in order to determine the possible inclusion mode of complexes. In this technique, the observation of ROESY cross-peaks indicates that the distance between the hydrogen nuclei from interest molecules are above 0.4 nm.[37] The protons labels of ABZ and S-β-CD and the ROESY spectrum of the system ABZ:S-β-CD are shown in Figure 3. The fact that the cross-peak between the internal S-β-CD protons and 'f' protons was stronger than the cross-peak observed with the 'e' protons and, also, the absence of correlation with 'g' protons, suggested that ABZ aromatic ring could be only partially included in the cavity. In addition, 'a' proton of ABZ interacts with Hα–α′ protons on the side chain of 6-*O*-β-CD derivative, indicating that the tail of ABZ was closer to the narrow opening of S-β-CD. These results indicated that the non-polar portion of the guest structure was encapsulated. An intermolecular cross peak was not observed between the 'd' protons and the internal protons of S-β-CD, thus, the head of the ABZ was probably outside the S-β-CD cavity.

Proton Hα–α′ presented a cross peak in the region corresponding to H3, H5 and H6. This could be due to the proximity of the succinyl group to the unsubstituted glucopiranose units.

The relative abundances and stoichiometries of the inclusion complex ABZ:S-β-CD (SD) were determined by ESI-MS in negative mode. The molecular ions with *m*/*z* at 748.8, 798.8, 848.8 and 898.7 corresponded to doubly charged species that may be attributed to the inclusion complex formed in an equimolar ratio between ABZ and S-β-CD presenting different DS (1–4 substituents). No signals were observed with a ratio *m*/*z* related to other complex stoichiometries. These results were in agreement with the ones obtained from the solubility diagrams. Ions with *m*/*z* at 748.8, 798.8, 848.8 and 898.7 were analyzed by MS–MS. The fragmentation of those ions produced certain ions, which corresponded to ABZ and the CD derivatives.

The morphology of ABZ, S-β-CD; and ABZ:S-β-CD systems prepared by PM or SD methods was investigated by means of an AMR 1000 Scanning Microscope (Amray, Bedford, MA). The samples were previously sputter-coated with a gold layer in order to make them conductive. Pictures were taken at an excitation voltage of 20 kV.

Figure 4 shows clearly that ABZ (a) is presented as small irregular particles (5–20 μm) while S-β-CD (b) existed in a mixture of different size and smooth-surface particles (10–300 μm). After observing the system ABZ:S-β-CD obtained by PM (c) both the ABZ and the S-β-CD kept their original morphology and size. On the other hand, when observing the system ABZ:S-β-CD obtained by SD (d) it was impossible to distinguish the presence of S-β-CD particles or ABZ crystals, showing a novel arrangement between ABZ and S-β-CD, which could correspond to the formation of an inclusion complex.

Fourier transform infrared (FT-IR) spectra were registered on a FT-IR-Prestige-21 Shimadzu (Tokyo, Japan). The KBr disk method (2 mg of each system in 100 mg KBr) was used for samples preparation. The scanning range was 450–3900 cm^{-1} with a resolution of 1 cm^{-1}. Figure 5 shows the following results: ABZ spectrum presents characteristic peaks at: 3332 cm^{-1} (N–H stretching of amine); 2954 and 2927 cm^{-1} (CH_3/CH_2 stretching of alkane); 2661 (C–H stretching of alkane); 1712 cm^{-1} (amide I band); 1631 cm^{-1} (aromatic ring stretching); 1589 cm^{-1} (aromatic C–N stretching) and 1523 cm^{-1} (amide II band).[38] The S-β-CD showed three major peaks: a broad peak at 3414 cm^{-1} (OH stretching), and two peaks at 2927 cm^{-1} (CH stretching) and at 1734 cm^{-1} corresponding to an ester group (which was formed by the reaction between carboxyl groups of the succinic acid and hydroxyl groups of the β-CD). The spectrum of ABZ:S-β-CD (PM) clearly exhibited the peaks corresponding to the samples of ABZ and S-β-CD and no shifting could be observed. In the spectrum of ABZ:S-β-CD obtained by SD, only some peaks could be detected in accordance with ABZ patterns (for example, 1632 cm^{-1} corresponding to the carbonyl group). This fact could indicate the load of ABZ in the inclusion complex.

Powder X-ray diffraction (XRD) measurements were performed on an automated X'Pert Phillips MPD diffractometer (Eindhoven, The Netherlands) using CuKα radiation (λ = 1.54056 Å), and

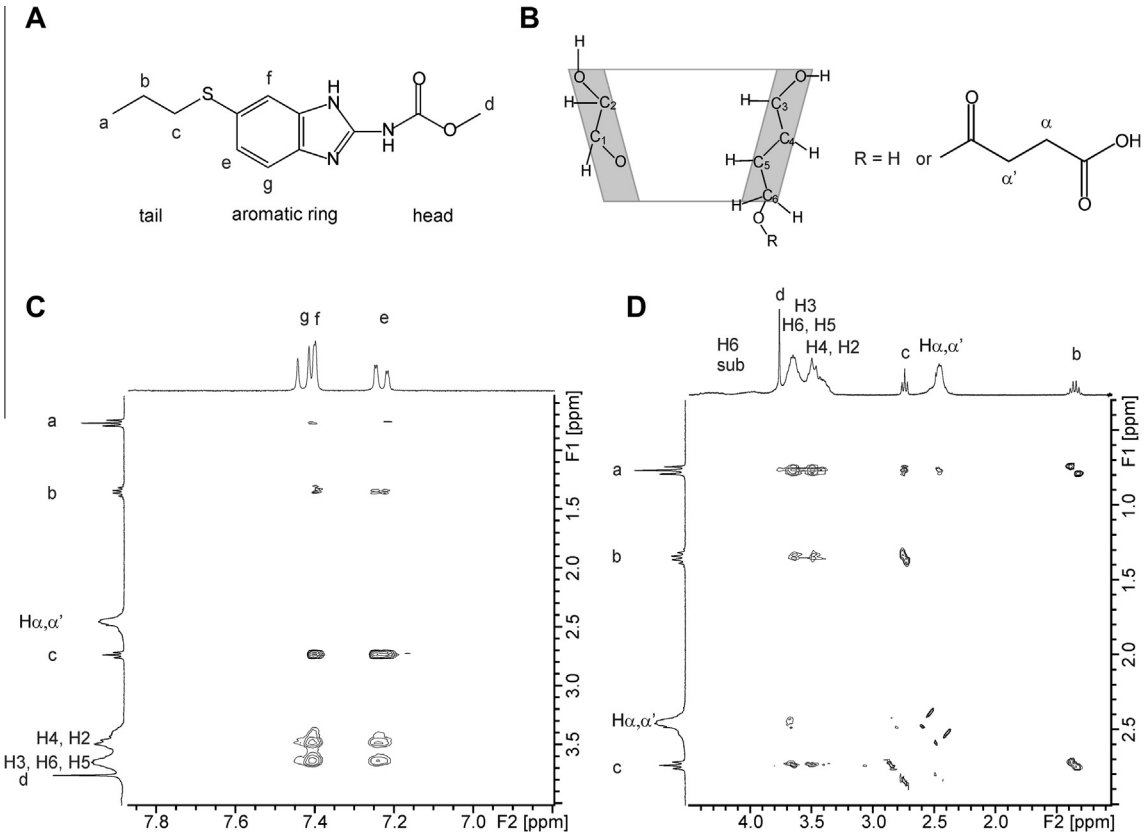

Figure 3. ROESY spectrum. (A) ABZ proton labelling, (B) S-β-CD proton labelling. (C) and (D) plot of two dimensional ROESY spectrum of ABZ in the presence of S-β-CD.

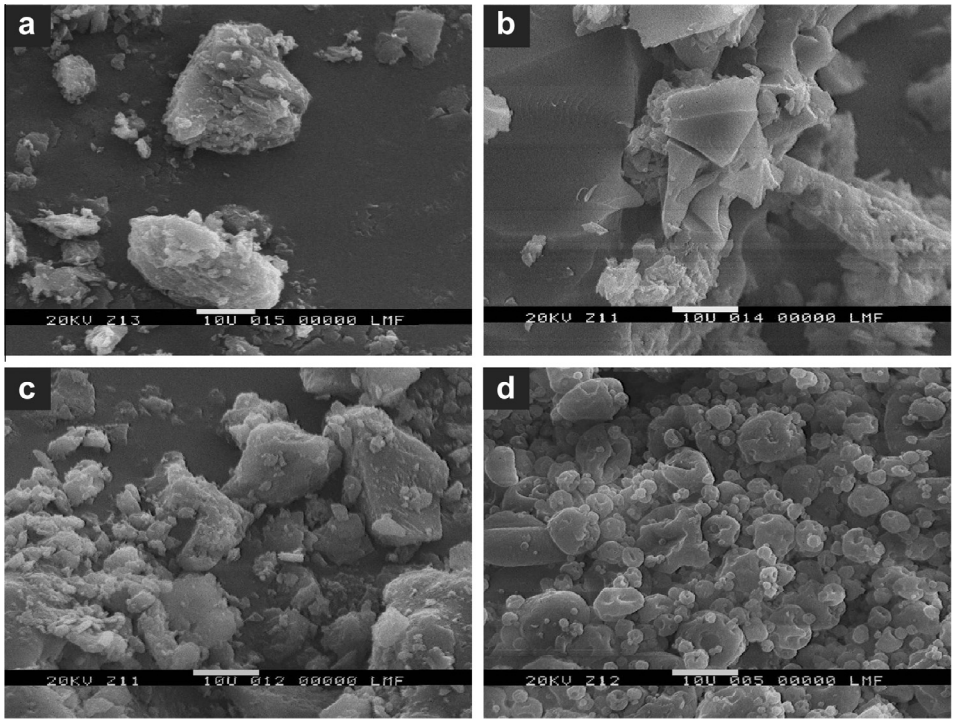

Figure 4. SEM micrographs of (a) ABZ (pure drug), (b) S-β-CD, (c) ABZ:S-β-CD obtained by PM, (d) ABZ:S-β-CD obtained by SD.

operating at 40 kV, 30 mA. Diffraction data were obtained with a step size of 0.02° over the 10–40° 2θ range. Low peak broadening and background were resolved by using parallel beam geometry by means of an X-ray lens and a graphite monocromator placed in front of the detector window. Data acquisition and evaluation were performed with the Stoe Visual-Xpow package, Version

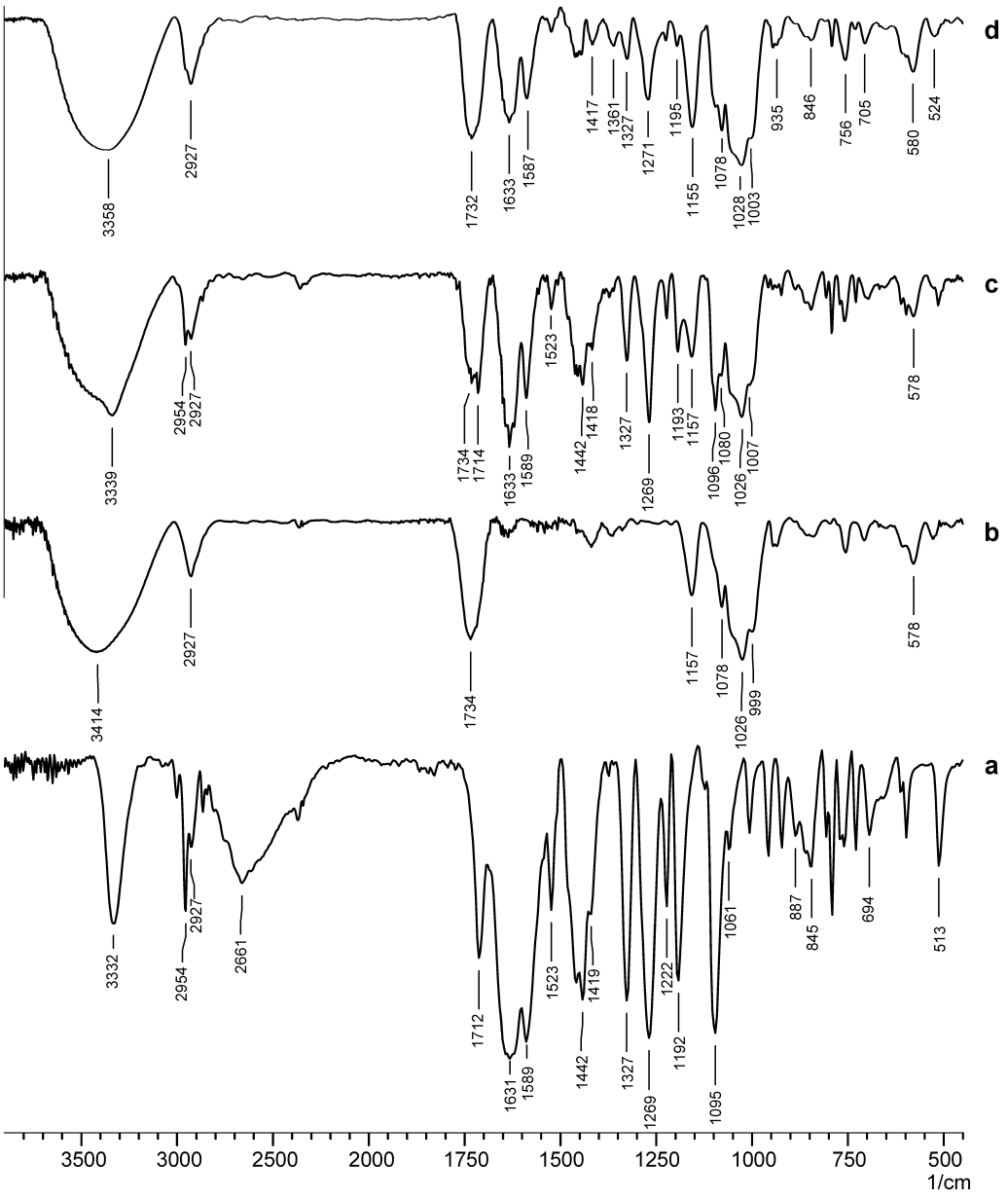

Figure 5. FT-IR. (a) ABZ (pure drug), (b) S-β-CD, (c) ABZ:S-β-CD obtained by PM, (d) ABZ:S-β-CD obtained by SD.

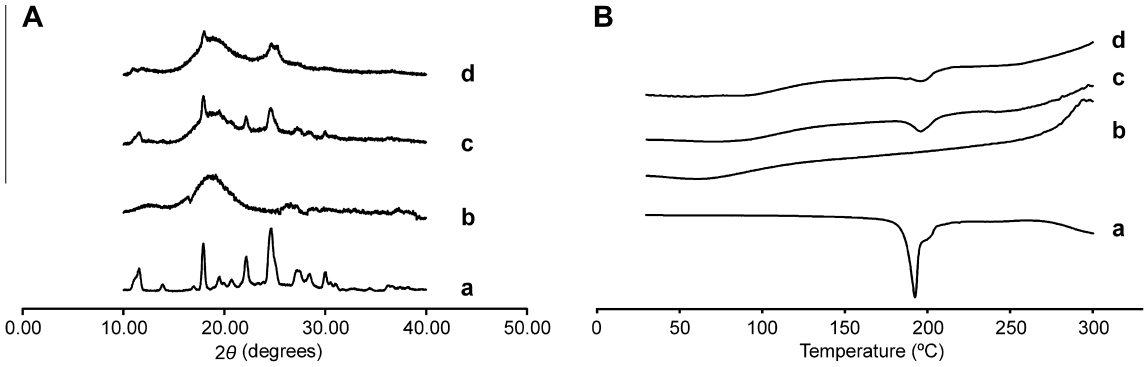

Figure 6. (A) XRD patterns. a: ABZ (pure drug), b: S-β-CD, c: ABZ:S-β-CD obtained by PM, d: ABZ:S-β-CD obtained by SD. (B) DSC thermograms. a: ABZ (pure drug), b: S-β-CD, c: ABZ:S-β-CD obtained by PM, d: ABZ:S-β-CD obtained by SD.

2.75 (Germany). Figure 6 A shows the analyses of the solid structure by XRD studies of ABZ, CD derivative and the systems prepared by PM and SD. ABZ presents intense and characteristic peaks at 2θ 11.51; 17.85; 22.09 y 24.54. On the other hand, S-β-CD shows an amorphous structure. The diffraction patterns of ABZ:S-β-CD obtained by PM shows the characteristic peaks of ABZ (2θ 11.51; 17.85; 22.09 y 24.54) with smaller intensity, which could be due to the dilution effect in the presence of the S-β-CD. Diffraction patterns of ABZ:S-β-CD obtained by SD showed only two weak peaks corresponding to ABZ at 2θ 17.85 and 24.54, which are broader and less intense, suggesting that ABZ is almost in an amorphous state. This result could be attributed to the partial complexation of ABZ in the S-β-CD cavity,[39] which is in agreement with the results obtained by IR.

Differential scanning calorimetry (DSC) was carried out on a Shimadzu TA-60 (Kyoto, Japan) calorimeter. The instrument was calibrated using indium and zinc as standards. Each sample (in crimped aluminium pan) was scanned at a rate of 5 °C/min from 30 to 300 °C, under N_2 atmosphere (flow rate 30 mL/min), and an empty aluminium pan was used as a reference. DSC thermograms of ABZ, S-β-CD and ABZ:S-β-CD prepared by PM and SD were carried out to analyze if modifications in the melting peak of ABZ had arisen when the drug was in combination with S-β-CD.[40] Figure 6 B demonstrated the characteristic sharp melting peak of ABZ at 196.84 °C. ABZ endothermic peak was also exhibited in PM systems, showing less intensity. The modification in the crystallinity structure of the drug loaded in the inclusion complex could be attributed to the influence on the manufacturing process produced by the SD method. These results were in agreement with those obtained by FT-IR and XRD analysis.

Equilibrium solubility: Excess of ABZ, ABZ:β-CD or ABZ:S-β-CD prepared by PM or SD method were placed into flasks which contain 10 mL of water (pH = 6.3) and shaken at 25.0 ± 0.5 °C for 72 h. After this time, the suspensions were filtered through a 0.45 μm membrane filter (Advantec MFS, Inc.) and ABZ concentrations were determined spectrophotometrically at 292 nm. Each experiment was performed in triplicate. The equilibrium solubility values of ABZ and the systems ABZ:β-CD and ABZ:S-β-CD obtained by PM and SD techniques are shown in Table 1. As it was observed, the solubility of ABZ raw material was 0.001 mg/mL. The use of β-CD allowed us to reach these solubility values: 0.013 mg/mL and 0.024 mg/mL preparing the systems by PM or SD methods, respectively. On the other hand, the solubility values obtained were 0.066 mg/mL (PM) and 0.224 mg/mL (SD), for the samples prepared with S-β-CD, indicating the efficacy of this derivative to increase the ABZ solubility. This enhancement in the ABZ solubility may be due to the interaction between the acidic groups of the S-β-CD and the basic groups of ABZ.

Dissolution studies were performed at 37 °C in HCl 0.1 N (900 mL), according to U.S. Pharmacopeia (USP)[41] Apparatus 2 (SR8 8-Flask Bath, Hanson Research, Chatsworth, CA) with paddle rotating at 50 rpm. Samples of ABZ raw material, PMs and inclusion complexes equivalent to 100 mg of ABZ were spread on the surface of the dissolution medium and the time 0 was recorded. At appropriate time intervals, 5 mL of samples were withdrawn and filtered (pore size 0.45 mm). The amount of drug released was determined spectrophotometrically at 292 nm. In addition, dissolution efficiency (DE) was calculated from the area under the dissolution curve at time and expressed as percentage of the area of the rectangle described by 100% dissolution.[42]

DE was calculated using Eq. 3:

$$DE = \frac{\int_0^t y \times dt}{y_{100} \times t} \times 100 \quad (3)$$

where y is the percentage of dissolved product at time. The dissolution profiles corresponding to ABZ:S-β-CD, ABZ:β-CD (obtained by SD or PM) and ABZ without any treatment are shown in Figure 7. The profiles of ABZ pure drug and ABZ:β-CD obtained by PM showed similar results, reaching only between 6% and 12% of drug release after 60 min of the running assay. Similar results were obtained after analyzing ABZ:β-CD (SD) and ABZ:S-β-CD (PM) profiles, achieving approximately 34% and 25% of drug released after 30 min (Q_{30}) and 46% and 44% of drug released after 60 min (Q_{60}). The dissolution behavior of the ABZ:S-β-CD (SD) inclusion complex, exhibited the highest drug released (95.5%) after 60 min of the running assay. The influence of the CD derivative in addition with the technological procedure (SD) increased particularly the drug release rate. In order to analyze differences between the dissolution rate profiles, DEs were calculated. This is a suitable parameter to compare in vitro dissolution profiles behavior of different formulations. The DE value at 360 min is shown in Table 1. As could be seen in Table 1 the DE of ABZ:S-β-CD (SD) achieved was 96.16% while ABZ only reached 11.94%. These results remarkably demonstrated the improvement of the dissolution rate of ABZ, loaded in this synthesized derivative S-β-CD.

In this work a S-β-CD derivative was synthesized in an aqueous medium starting from β-CD and succinic acid, in the presence of SHP. The reaction was performed under very mild conditions obtaining a very good yield. The reaction product was employed for the formulation of inclusion complex of ABZ, a poorly soluble compound use as a model drug. The derivative and the complex were completely characterized, verifying the inclusion of the drug in the CD cavity. Thus, the use of S-β-CD improved remarkably the ABZ physicochemical properties. Water solubility showed 200 fold increased, and the dissolution rate was complete after 60 min of the running assay.

Thus this non toxic derivative obtained by green synthesis could be a suitable excipient to design oral dosage forms, particularly for the treatment of parasitic diseases.

Table 1
Equilibrium solubility values, Q_{30} (%), Q_{60} (%) and dissolution efficiency percentages of ABZ (pure drug), ABZ:β-CD and ABZ:S-β-CD prepared by PM and SD

Systems		Solubility (mg/mL)	Q_{30} (%)	Q_{60} (%)	DE (%)
ABZ	—	0.001	3.8	6.1	11.9
ABZ:β-CD	PM	0.013	7.7	12.6	20.9
	SD	0.024	34.5	46.6	61.9
ABZ:S-β-CD	PM	0.066	25.2	44.3	61.1
	SD	0.224	91.8	95.5	96.1

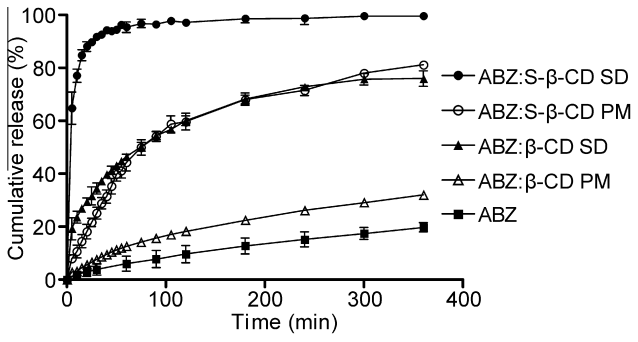

Figure 7. Dissolution profiles. Release profiles of ABZ (raw material), ABZ loaded in PMs (β-CD and S-β-CD), ABZ loaded in the inclusion complexes prepared by SD (β-CD and S-β-CD). Test conditions: 0.1 N HCl, 37 °C (n = 3, ±SD).

Acknowledgements

A.G. and is grateful to CONICET (Consejo Nacional de Investigaciones Científicas y Técnicas) for a Doctoral Fellowship.

The authors gratefully acknowledge the Universidad Nacional de Rosario and CONICET (Project N° PIP 112-201001-00194) for financial support.

We would like to thank Marcela Culasso, María Robson, Mariana de Sanctis, Carolina Perret and Geraldine Raimundo for their assistance in the correction of the language.

The authors also thank Ferromet S.A. (agent of Roquette in Argentina) for their donation of β-CD.

References and notes

1. Murrell, K. D. Helminthic Diseases: Trichinellosis and Zoonotic Helminthic Infections. In *International Encyclopedia of Public Health*; Heggenhougen, H. K., Ed.; Academic Press: Oxford, 2008; p 368.
2. Horton, R. J. *Parasitol. Today* **1990**, *6*, 106.
3. Kawabata, Y.; Wada, K.; Nakatani, M.; Yamada, S.; Onoue, S. *Int. J. Pharm.* **2011**, *420*, 1.
4. Leonardi, D.; Lamas, M. C.; Olivieri, A. C. *J. Pharm. Biomed. Anal.* **2008**, *48*, 802.
5. Leuner, C.; Dressman, J. *Eur. J. Pharm. Biopharm.* **2000**, *50*, 47.
6. García, A.; Leonardi, D.; Salazar, M. O.; Lamas, M. C. *PLoS One* **2014**, *9*, e88234.
7. García, A.; Leonardi, D.; Vasconi, M. D.; Hinrichsen, L. I.; Lamas, M. C. *PLoS One* **2014**, *9*, e113296.
8. García, A.; Barrera, M. G.; Piccirilli, G.; Vasconi, M. D.; Di Masso, R. J.; Leonardi, D.; Hinrichsen, L. I.; Lamas, M. C. *Parasitol. Int.* **2013**, *62*, 568.
9. Yuvaraja, K.; Khanam, J. *J. Pharm. Biomed. Anal.* **2014**, *96*, 10.
10. Lahiani-Skiba, M.; Bounoure, F.; Shawky-Tous, S.; Arnaud, P.; Skiba, M. *J. Pharm. Biomed. Anal.* **2006**, *41*, 1017.
11. Jansook, P.; Kurkov, S. V.; Loftsson, T. *J. Pharm. Sci.* **2010**, *99*, 719.
12. Kennedy, J. F.; Szymańska, A. *Carbohydr. Polym.* **2008**, *71*, 704.
13. Mura, P. *J. Pharm. Biomed. Anal.* **2014**, *101*, 238.
14. Mura, P. *J. Pharm. Biomed. Anal.* **2015**.
15. Dodziuk, H. *Molecules with Holes—Cyclodextrins, Cyclodextrins and Their Complexes*; Wiley-VCH Verlag GmbH & Co. KGaA, 2006. p 1.
16. Szejtli, J. *J. Mater. Chem.* **1997**, *7*, 575.
17. Vogt, F. G.; Strohmeier, M. *Mol. Pharm.* **2012**, *9*, 3357.
18. Yuan, C.; Liu, B.; Liu, H. *Carbohydr. Polym.* **2015**, *118*, 36.
19. Zhou, Q.; Wei, X.; Dou, W.; Chou, G.; Wang, Z. *Carbohydr. Polym.* **2013**, *95*, 733.
20. Lang, W.; Kumagai, Y.; Sadahiro, J.; Maneesan, J.; Okuyama, M.; Mori, H.; Sakairi, N.; Kimura, A. *Bioresour. Technol.* **2014**, *169*, 518.
21. Balducci, A.; Magosso, E.; Colombo, G.; Sonvico, F.; Khan, N.; Yuen, K.; Bettini, R.; Colombo, P.; Rossi, A. *AAPS PharmSciTech* **2013**, *14*, 911.
22. Davis, M. E.; Brewster, M. E. *Nat. Rev. Drug Disc.* **2004**, *3*, 1023.
23. Loftsson, T.; Brewster, M. E. *J. Pharm. Sci.* **1996**, *85*, 1017.
24. Loftsson, T.; Brewster, M. E. *J. Pharm. Sci.* **2012**, *101*, 3019.
25. Challa, R.; Ahuja, A.; Ali, J.; Khar, R. K. *AAPS PharmSciTech* **2005**, *6*, E329.
26. Schonbeck, C.; Westh, P.; Madsen, J. C.; Larsen, K. L.; Stade, L. W.; Holm, R. *Langmuir* **2011**, *27*, 5832.
27. Khan, A. R.; Forgo, P.; Stine, K. J.; D'Souza, V. T. *Chem. Rev.* **1998**, *98*, 1977.
28. Hattori, K.; Ikeda, H. *Modification Reactions of Cyclodextrins and the Chemistry of Modified Cyclodextrins, Cyclodextrins and Their Complexes*; Springer, 2006. p 31.
29. Sadeghian, H.; Jabbari, A. Amphiphilic Cyclodextrins, Synthesis, Utilities and Application of Molecular Modeling in Their Design. In *Recent Advances in Novel Drug Carrier Systems*; Ali Demir Sezer Ed.; InTech, 2012. http://dx.doi.org/10.5772/50220.
30. Cucinotta, V.; Giuffrida, A.; Maccarrone, G.; Messina, M.; Puglisi, A.; Torrisi, A.; Vecchio, G. *J. Pharm. Biomed. Anal.* **2005**, *37*, 1009.
31. Fernández, M.; Fragoso, A.; Cao, R.; Baños, M.; Ansorge-Schumacher, M.; Hartmeier, W.; Villalonga, R. *J. Mol. Catal. B: Enzym.* **2004**, *31*, 47.
32. Uekama, K.; Hirayama, F.; Arima, H. *Pharmaceutical Applications of Cyclodextrins and Their Derivatives, Cyclodextrins and Their Complexes*; Wiley-VCH Verlag GmbH & Co. KGaA, 2006. p 381.
33. Dodziuk, H.; Hashimoto, H.; Morillo, E.; Bilewicz, R.; Chmurski, K. *Applications Other than in the Pharmaceutical Industry, Cyclodextrins and Their Complexes*; Wiley-VCH Verlag GmbH & Co. KGaA, 2006. p 450.
34. Higueras, L.; López-Carballo, G.; Cerisuelo, J. P.; Gavara, R.; Hernández-Muñoz, P. *Carbohydr. Polym.* **2013**, *97*, 262.
35. Yu, Q.; Black, S.; Wei, H. *J. Chem. Eng. Data* **2009**, *54*, 2123.
36. Higuchi, T.; Connors, K. A. *Adv. Anal. Chem. Inst.* **1965**, *4*, 117.
37. Schneider, H. J.; Hacket, F.; Rudiger, V.; Ikeda, H. *Chem. Rev. (Washington, D.C.)* **1998**, *98*, 1755.
38. Gunasekaran, S.; Uthra, D. *Asian J. Chem.* **2008**, *20*, 6310.
39. Ogawa, N.; Takahashi, C.; Yamamoto, H. *J. Pharm. Sci.* **2015**, *104*, 942.
40. Miller, L. A.; Carrier, R. L.; Ahmed, I. *J. Pharm. Sci.* **2007**, *96*, 1691.
41. United States Pharmacopeia, USP, Rockville (MD), 2009.
42. Rudrangi, S. R. S.; Trivedi, V.; Mitchell, J. C.; Wicks, S. R.; Alexander, B. D. *Int. J. Pharm.* **2015**, *494*, 408.